Large Sign Language Models: Toward 3D American Sign Language Translation

Sen Zhang^{1*} Xiaoxiao He^{1*} Di Liu² Zhaoyang Xia¹ Mingyu Zhao¹ Chaowei Tan³ Vivian Li⁶ Bo Liu⁴ Dimitris N. Metaxas² Mubbasir Kapadia⁵

¹Rutgers University ²Meta Reality Labs ³Qualcomm ⁴Walmart Global Tech

⁵Roblox ⁶PRISMS

Abstract

We present Large Sign Language Models (LSLM), a novel framework for translating 3D American Sign Language (ASL) by leveraging Large Language Models (LLMs) as the backbone, which can benefit hearing-impaired individuals' virtual communication. Unlike existing sign language recognition methods that rely on 2D video, our approach directly utilizes 3D sign language data to capture rich spatial, gestural, and depth information in 3D scenes. This enables more accurate and resilient translation, enhancing digital communication accessibility for the hearing-impaired community. Beyond the task of ASL translation, our work explores the integration of complex, embodied multimodal languages into the processing capabilities of LLMs, moving beyond purely text-based inputs to broaden their understanding of human communication. We investigate both direct translation from 3D gesture features to text and an instruction-guided setting where translations can be modulated by external prompts, offering greater flexibility. This work provides a foundational step toward inclusive, multimodal intelligent systems capable of understanding diverse forms of language.

1. Introduction

Sign languages are vital as they are the primary means of communication for hundreds of millions of hearing-impaired individuals globally [11]. Bridging the communication gap between sign language users and the non-signing majority is crucial for fostering inclusivity in education, employment, and daily social interactions. Recent advancements in deep learning and natural language processing have paved the way for developing automated sign language understanding and translation systems [6, 12, 20, 33–35, 57, 58], aiming to enhance accessibility and facilitate seamless communication. However, existing approaches relying on 2D video are inherently vulnerable to variations in camera view angles, lighting conditions, and complex backgrounds, which can

degrade performance in 3D virtual environment scenarios and often necessitate constrained, simplified environments [9, 21–23, 27, 28, 40, 42, 50, 61, 62]. Concurrently, Large Language Models (LLMs) have demonstrated remarkable capabilities in understanding, generating, and translating textual languages. This success has spurred research into extending LLM capabilities to multimodal domains, including the interpretation of visual data. As highlighted by recent studies, efforts are underway to integrate LLMs for gloss-free sign language translation directly from video, aiming to leverage their extensive linguistic knowledge to produce more coherent and contextually appropriate translations [1, 16, 26, 55].

While prior work has predominantly relied on 2D video data for sign language translation, such approaches are constrained by fixed camera perspectives, simplified backgrounds, and limited spatial understanding [7, 10, 14, 15, 19, 29–31, 36–39, 44, 54, 59, 60]. To address these limitations for virtual communication, we propose a 3D-based approach that leverages rich motion representations encoded via SMPL-X [47], as provided by recent 3D sign language datasets [56]. These 3D representations offer detailed articulations of the body and hands, enabling more accurate modeling of the complex spatio-temporal patterns inherent in signing. Moreover, insights from LLM-driven human motion understanding and synthesis [25, 53] highlight the potential of combining temporal dynamics with large-scale language priors to interpret embodied communication. Ultimately, 3D sign language understanding not only enhances translation robustness but also enables hearing-impaired communication in virtual environment.

In this paper, we introduce the *Large Sign Language Model (LSLM)*, a novel framework that harnesses the capabilities of large language models (LLMs) for translating 3D American Sign Language (ASL). Unlike traditional approaches that rely on 2D video data, our method leverages 3D gesture features derived from detailed body and hand motion. By interfacing these 3D motion representations with an LLM backbone, LSLM enhances translation robustness and accuracy for hearing-impaired users. More broadly, our

^{*}Equal contribution.

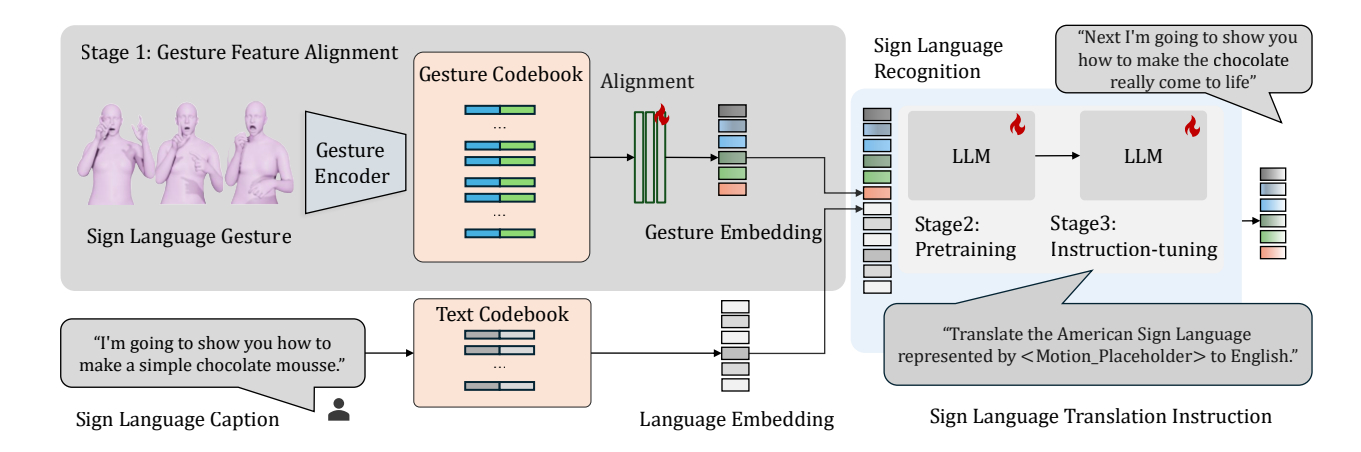


Figure 1. The training pipeline for our Large Sign Language Model (LSLM) initiates with a pretrained text-based large language model and proceeds in three stages. First, we train a motion vector-quantized variational autoencoder (VQ-VAE); its quantized outputs are then used with a projection layer for gesture-text alignment. Second, these aligned gesture features serve as input to pretrain the LLM, enabling foundational sign language understanding. Finally, the model is instruction-finetuned to develop its ability to follow instructions with sign language.

work contributes to the emerging field of embodied multimodal understanding, expanding LLM capabilities beyond text to encompass complex, physical forms of human communication such as sign language.

Our contributions are threefold. **First**, we propose a novel framework for aligning 3D sign language representations with LLMs to enable end-to-end translation. **Second**, we explore direct translation from 3D gesture features to textual output, bypassing traditional gloss-based intermediates and reducing annotation dependency. **Third**, we introduce an instruction-guided translation setting that allows the model to adapt its outputs based on external prompts, offering greater flexibility and contextual awareness. Together, these advances represent a foundational step toward building inclusive, generalizable, and intelligent systems for sign language understanding and communication.

2. Related Works

2.1. Sign Language Recognition

Sign Language Recognition (SLR) has transitioned from sensor-based methods to robust, video-based deep learning frameworks for continuous signing, enabled by prevalent high-resolution video and affordable cameras. Computer vision techniques now extract crucial manual and nonmanual features (e.g., hand shape, facial expressions) [2]. Early methods combining handcrafted features with Hidden Markov Models (HMMs) for spatio-temporal modeling were superseded by deep Convolutional Neural Networks (CNNs) for spatial feature extraction and Recurrent Neural Network (RNN)/Long Short-Term Memory (LSTM) models for temporal modeling [8, 27]. Quantitative surveys document SLR's progression towards advanced deep learning

architectures using full-frame video, iterative optimization, and data augmentation, enabling robust signer-independent recognition in unconstrained environments [9, 27].

2.2. Sign Language in Large Language Models

Recent video-based Sign Language Recognition (SLR) research integrates Large Language Models (LLMs) for glossfree translation, bridging visual input and semantic language output [1, 16]. This paradigm employs transformer-based architectures to convert continuous sign videos directly into discrete token sequences, bypassing intermediate gloss annotations. Visual encoders compress spatio-temporal features into language-like representations [1, 16]. Innovations like the Vector-Quantized Visual Sign (VQ-Sign) module transform video inputs into character-level tokens via discrete codebook reconstruction and alignment, mitigating the visual-text modality gap and providing LLMs with structured input for leveraging their linguistic knowledge [16, 26]. This gloss-free approach enables LLMs to resolve ambiguities and generate coherent translations from visual data, leading to scalable sign language translation systems [1, 5]. LLM integration signifies a paradigm shift, enabling seamless video-to-spoken language conversion by harnessing extensive textual understanding previously inaccessible to visiononly models [5, 16].

2.3. LLM-based Motion Understanding

Recent advancements have seen the application of large language models (LLMs) to human motion synthesis. MotionGPT [25] treats the discrete tokens as context-free, raw indicators of motion which are then dynamically reinterpreted within subsequent generative modules. This design choice facilitates a more fluid and context-adaptive recon-

struction process, one in which the generative network is free to reconstruct and refine motion details based solely on the current context and temporal requirements rather than being tethered to static, pre-learned representations. Such an approach is particularly beneficial in capturing the subtle nuances of signing—where minor variations in gesture intensity, duration, and transition phases can alter meaning—and serves to better accommodate inter-signer variability and environmental noise. Through such innovative synthesis, MotionGPT-type architectures [25, 53] demonstrate significant promise in advancing the state-of-the-art in sign language recognition. Thus, we proposed Large Sign Language Model (LSLM), a novel framework specifically designed to adapt and extend these advanced motion-language principles to the unique challenges of this domain. Our LSLM focuses on interpreting the complex spatio-temporal dynamics and grammatical structures inherent in sign languages, by leveraging fine-grained motion representations inspired by these architectures and the contextual understanding capabilities of large language models, to achieve robust translation from sign inputs to spoken or written text.

3. Methods

To enable sign language understanding, our method leverages the intrinsic linguistic knowledge of Large Language Models (LLMs). We address two primary technical challenges: 1) existing methods utilizing video as inputs are inefficient and cannot generalize to different camera angles or backgrounds; 2) the generation of sign language representations suitable for direct integration with LLM architectures. The subsequent subsections detail our proposed model architecture (Fig. 1) and the training strategy designed to overcome these challenges.

3.1. Environment Agnostic 3D Sign Language Tokenization

Existing work, such as that by Gong et al. [16], often utilizes direct video feed as input for language models. While achieving commendable results on specific test datasets, these approaches can be susceptible to variations in visual artifacts or background changes, potentially leading to drastic fluctuations in the vision encoder's output. Furthermore, datasets used for training such models may exhibit strong consistency in camera angles, introducing a bias that can limit generalization. To address these challenges and enable sign language translation that is robust against domain shifts, we propose a sign language tokenizer centered on 3D skeletal data.

SMPL-X is a comprehensive, unified 3D model of the human body that distinctly represents the body, face, and hands together. SMPL-X features 10, 475 vertices and 54 joints, which include articulations for the neck, jaw, eyeballs, and fingers, allowing for a richer representation of human motion and expression. However, in our sign language application,

the two joints corresponding to the eyeballs are excluded, leading to the use of 52 joints for pose parameterization. The model is parameterized by pose, shape, and facial expression parameters, enabling fine-grained control over the generated 3D human mesh. This is especially Assuming the availability of accurate 3D skeleton extraction from arbitrary video input, our core contribution is a vector quantized variational autoencoder (VQVAE)-based sign motion encoder. This encoder is designed to transform continuous sign language motion sequences into a discrete sequence of tokens. With existing SMPL-X parameter estimators [3], we are able to extract the human pose motion from a sign video and then utilize the motion representations for sign language understanding.

Our sign language tokenizer architecture, inspired by recent advancements in motion representation [25], consists of an encoder (\mathcal{E}) and a decoder (\mathcal{D}) . The encoder (\mathcal{E}) takes a sequence of SMPL-X 3D skeleton representation, representing M frames of human motion $(s^{1:M})$ to obtain latent vectors. These latent vectors $(\hat{z}^{1:L})$ are then subjected to a vector quantization process $(Q(\cdot))$. This involves a learnable codebook $C = \{c^k\}_{k=1}^K$, which contains K latent embedding vectors, each of dimension d. Each latent vector \hat{z}^i is mapped to its nearest codebook entry $c_k \in C$, resulting in a sequence of discrete motion tokens $z^{1:L}$, where L is the downsampled length of the token sequence.

$$z^{1:L} = Q(z^{\hat{1}:L}) = \min_{c_k \in C} ||\hat{z}^i - c_k||_2 \tag{1}$$

The decoder (\mathcal{D}) is then trained to reconstruct the original motion sequence $\hat{m}^{1:M}$ from these discrete tokens $z^{1:L}$. The training of the VQVAE involves a combination of reconstruction loss, an embedding loss to update the codebook vectors, and a commitment loss to ensure the encoder outputs commit to specific codebook entries [18, 51], defined in equation (2), where $\mathrm{sg}[\cdot]$ denotes the stop-gradient operation, and β is a weighting factor.

3.2. Sign Language Motion to Text Alignment

Using this Sign Language tokenizer, we are able to encode the Sign Language to a sequence of quantized representations. However, for a pre-trained large language model (LLM) to understand and use sign language for applications, it needs to comprehend sign motion. The initial quantized embeddings from the tokenizer are not compatible with the word embeddings that the pre-trained LLM understands. Therefore, an alignment process is necessary. In our work, we utilize 2 multilayer perceptron (MLP) $\phi(\cdot)$ to align the quantized representation to the input embeddings of the LLM. After this mapping, these aligned embeddings $E_{sign}^{1:L} = \phi(z^{1:L})$ can be fused with the language embeddings E_{lang} and feed into the Large Language Model, enabling it to process and understand the sign language input for tasks such as translation or recognition.

$$\mathcal{L}_{vq} = ||\hat{s}^{1:M} - s^{1:M}||_1 + ||\operatorname{sg}[\mathcal{E}(s^{1:M})] - z^{1:L}||_2^2 + \beta||\mathcal{E}(s^{1:M}) - \operatorname{sg}[z^{1:L}]||_2^2$$
(2)

Table 1. Quantitative results for sign language recognition during the pretraining stage. MLP: Direct Alignment and Fusion; MLP+LLM: Joint training; MLP/LLM: Staged training.

Methods	Pretraining	Bleu@1↑	Rouge↑	CIDEr↑
MotionGPT	-	7.9	8.3	2.5
Ours (Direct Alignment and Fusion)	MLP	12.1	10.2	23.4
Ours (Joint pretraining)	MLP+LLM	13.6	11.7	26.9
Ours (Staged pretraining)	MLP/LLM	14.0	11.7	20.7

3.3. Training Scheme

The training process is divided into three stages. The first stage is Sign Language Tokenizer training, which focuses on reconstructing the sign clips as discrete tokens. The second stage is Modality-Alignment Pre-training, which aims to align the sign language space with pretrained text representation and facilitate collaboration across the SLR task. The third stage is Instruction Fine-Tuning, aimed at enhancing the model's instruction-following capability.

Sign Language Tokenizer Training. The initial phase involves the training of the Sign Language tokenizer. Upon successful training, any given sign language motion sequence, denoted as $s^{1:M}$, can be effectively represented as a corresponding sequence of motion tokens. Once this training stage is complete, the parameters of the motion tokenizer are fixed and remain unchanged throughout all subsequent stages of the processing pipeline.

Pretraining. The Llama models are trained and fine-tuned on natural language datasets. To enable these large language models to comprehend sign language, our methodology begins by first aligning motion embeddings from the sign language tokenizer with corresponding text embeddings through a dedicated training phase. Following this crucial alignment, we then continue to pre-train these models. This stage of pre-training utilizes the aligned sign language data and the corresponding text translation, with the specific aim of embedding sign language recognition capabilities within the large language models. For an input motion $s^{1:M}$, we consider the motion encoder trained from the previous section, which provides the motion feature $z^{1:L} = \mathcal{E}(s^{1:M})$. In this stage, Data was prepared in Gesture and Annotation pairs following the format presented in MotionGPT [25].

Instruction Tuning. To enhance the translation of sign language into text, we developed an instruction-tuned dataset specifically for the sign language to text. This dataset was constructed by leveraging sign language corpora and reformulating the translation objective within an instruction-following paradigm, building upon foundational methodologies observed in text-motion alignment from broader motion

capture research. Our focus is on the core task of converting sign language sequences into their corresponding textual representation. To this end, we composed dozens of varied instruction templates to promote robustness and prompt diversity. This process yielded a substantial collection of unique instructional prompts, each soliciting the spoken/written language equivalent of a given sign language sequence. Similar to the pretrain stage, we generate instructional ASL translation templates based on MotionGPT [25]. Please refer to List 1 in the appendix for examples.

4. Experiments

4.1. Experimental Setup

Datasets and Preprocessing. We utilize the American Sign Language subset of SignAvatars [56], which provides 3D sign language motion sequences across multiple languages with corresponding text annotations, and statistical information is shown in Tab 10 in the appendix. How2Sign dataset contains over 30000 samples, and we divided the dataset into 80% training set, 10% test, and validation set. The 3D motion is represented via the SMPL-X model, using 52 joints for body and hand kinematics. Following the HumanML3D [17] processing methodology, we extract a 623-dimensional feature vector per frame. This vector encodes root velocity, local joint positions, and local joint rotations, serving as the input representation for our model.

Evaluation Metrics. We evaluate translation quality using metrics standard in sign language and motion-to-text

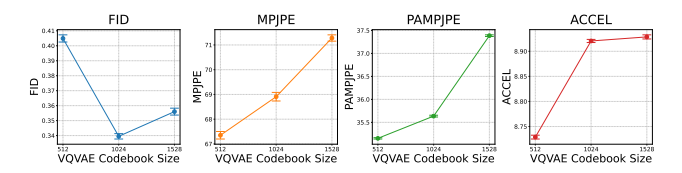


Figure 2. Evaluation of VQ-VAE codebook sizes on the How2Sign 3D dataset. A codebook size of 1024 offers the best trade-off, achieving the lowest FID while maintaining competitive MPJPE and PAMPJPE scores.

Table 2. Quantitative results for sign language recognition during the instruction-tuning stage. MLP: Direct Alignment and Fusion; MLP+LLM: Joint training.

Methods	Pretrained Modules	Instruction Tuning	Bleu@1↑	Rouge↑	CIDEr↑
MotionGPT	-	-	2.5	2.4	$5.7 \times e^{-4}$
Ours	MLP	LLM	14.2	11.9	28.0
Ours	MLP	MLP+LLM	13.8	11.7	21.0
Ours	MLP+LLM	LLM	14.1	11.5	20.6
Ours	MLP+LLM	MLP+LLM	14.1	11.2	27.3

research, following practices in works [1, 5, 8, 9, 16, 26, 27] and MotionGPT [25]. We report Word Error Rate (WER) to measure lexical accuracy against reference translations (lower is better). Additionally, we utilize the established linguistic metrics BLEU [46], ROUGE-L [32], and CIDEr [52] to assess translation fluency, content overlap, and semantic similarity, respectively.

Implementation Details. For gesture tokenization, we set the codebook size to 1024. This value was empirically determined to provide the optimal balance for reconstruction quality, achieving the lowest Fréchet Inception Distance (FID) while maintaining favorable Mean Per Joint Position Error (MPJPE) and Percentage of Accelerated MPJPE (PAMPJPE), with detailed metric comparisons presented in Fig. 2. The gesture tokenizer was trained using the AdamW optimizer [41] with a learning rate of 2×10^{-4} and a batch size of 256. In the subsequent gesture-language alignment stage, Llama-3.2-3B-Instruct [45] was employed as the large language model backbone, and we set learning rate to 1×10^{-6} for modality alignment, and 5×10^{-7} for LLM backbone fine-tuning. Our experiments are conducted on 8 Nvidia A100 GPUs.

4.2. Comparison with Motion-to-Text Approaches

To establish a baseline for Sign Language Recognition (SLR) task, we adapted the Motion-to-Text (M2T) capabilities of the MotionGPT framework [25], training it on 3D American Sign Language (ASL) data. This adaptation is motivated by the inherent structural similarity between M2T and SLR, as both tasks involve translating sequences of motion or gesture into textual output. However, a crucial distinction lies in the semantic nature of the target text: M2T typically aims to generate descriptive captions of the observed motion, whereas SLR endeavors to produce direct and accurate translations of the signed gestures.

As shown in Table 1, our proposed Large Sign Language Model (LSLM) consistently outperforms the adapted MotionGPT baseline across all pretraining metrics. This superior performance underscores LSLM's enhanced capacity for comprehending the complex nuances of ASL gesture modality, which consequently leads to the generation of more accurate translations. Two key architectural differences contribute to this performance gain. 1) Enhanced Motion Representation: Unlike MotionGPT, which directly inputs

discrete motion tokens into its LLM backbone, LSLM utilizes gesture embeddings derived after the initial tokenization process. 2) Explicit Modality Alignment: LSLM incorporates a dedicated modality alignment mechanism, i.e., Direct Alignment and Fusion. This component is designed to map the learned embeddings from the gesture space to the text embedding space of the Llama LLM backbone, facilitating a more effective and coherent integration of visual-gestural information with the language model's existing linguistic knowledge.

We further compare the models under instruction-following conditions, with results summarized in Table 2. Following the initial pertaining, LSLM demonstrated effective instruction fine-tuning, evidenced by a consistent improvement in performance metrics compared to its pre-instruction fine-tuning state. In stark contrast, the MotionGPT baseline exhibited a degradation in performance after its instruction fine-tuning phase. This divergence indicates the superior adaptability and effectiveness of our LSLM framework in leveraging instructional cues for the nuanced task of sign language translation, further validating our architectural and training choices.

4.3. Modality Alignment and Pretraining

To determine the most effective training scheme for aligning the gesture modality with the Large Language Model (LLM) backbone in the end-to-end Sign Language Recognition (SLR) task, we conducted three ablation studies. For these experiments, the data were structured as gesture-translation pairs, prepared according to the procedures detailed in Section 3.3, which is also happens to be the format of Direct Sign Language Recognition. The following three training schemes were systematically investigated: 1) Direct Alignment and Fusion: This approach involved a straightforward alignment of the gesture feature space with the text embedding space using a Multi-Layer Perceptron (MLP). The resulting gesture embeddings were then fused with the LLM's input embeddings for processing by the LLM backbone. 2) Joint pretraining: In this scheme, both the MLP (for gesture-to-text space alignment) and the entire LLM backbone were jointly pretrained. This was performed using the paired gesture and textual annotation data, allowing for simultaneous optimization of both the gesture processing component and the language model. 3) Staged pretraining:

Table 3. Ablation studies of the pretrain scheme for the Sign Language Recognition. MLP: Direct Alignment and Fusion; MLP+LLM: Joint training; MLP/LLM: Staged training.

Pretraining	Bleu@1↑	Bleu@4↑	Rouge↑	CIDEr↑	WER↓	Insertions↓	Deletions↓
MLP	12.1	1.0	10.2	23.4	140	4.2	4.0
MLP+LLM	13.6	1.5	11.7	26.9	114	4.0	1.7
MLP/LLM	14.0	1.6	11.7	20.7	118	3.9	1.4

Table 4. Ablation studies of the instruction-tuning scheme for the Sign Language Recognition. MLP: Direct Alignment and Fusion; MLP+LLM: Joint training.

Pretraining	Instruction Tuning	Bleu@1↑	Bleu@4↑	Rouge↑	CIDEr↑	WER↓	Insertions↓	Deletions↓
MLP	LLM	14.2	1.6	11.9	28.0	146	4.0	1.0
MLP	MLP+LLM	13.8	1.5	11.7	21.0	149	4.4	0.9
MLP+LLM	LLM	14.1	1.5	11.5	20.6	141	3.4	1.2
MLP+LLM	MLP+LLM	14.1	1.5	11.2	27.3	132	3.0	1.4

This method adopted a two-stage process. Initially, the MLP was pretrained to learn the mapping from gesture features to an intermediate representation aligned with the LLM's embedding space. Subsequently, during the second stage, the LLM backbone was pretrained on the translation task while the parameters of the pretrained MLP were kept frozen.

The outcomes of our ablation studies, detailed in Table 3, provide insights into the efficacy of different training schemes. The Direct Alignment and Fusion approach yielded decent results over the baseline. This initial success indicates the importance and effectiveness of explicitly aligning the gesture modality with the LLM's textual embedding space. But compared to the latter two schemes, this scheme generates redundant words as the deletion is higher. Building upon this observation, the Joint Petraining scheme demonstrated further improvements in textual similarity metrics, notably BLEU, ROUGE, and WER. This suggests that allowing the LLM to adapt concurrently with the gesture modality facilitates a more refined translation output. Conversely, the Staged Pretraining approach, while conceptually sound, resulted in a discernible decrease in semantic similarity scores (e.g., CIDEr), indicating that freezing the MLP after pretraining may restrict the LLM's ability to fully leverage the learned gesture representations during its own fine-tuning phase. Considering the overall balance of performance across all metrics, we selected the Joint Pretraining strategy as the optimal configuration for LSLM on the SLR task. Approach 1 and 3 checkpoints were subsequently employed for further instructional experiments and evaluations.

4.4. Instruction Finetuning

To further enhance the versatility and applicability of LSLM beyond direct translation, we incorporated an instruction fine-tuning stage. This stage aims to enable the model to perform the sign language recognition task in response to

varied explicit instructions, thereby broadening its utility for more diverse interactive scenarios. For this purpose, we adapted instruction templates originally proposed in MotionGPT [25]. These templates, initially designed for general, descriptive motion, were systematically transformed into formats suitable for ASL translation tasks, as detailed in Section 3.3. To identify the optimal approach for this stage, we also conducted a series of ablation studies focused on different fine-tuning schemes specifically for instruction following.

Further analysis of instruction fine-tuning strategies, with results detailed in Table 4, revealed interesting trade-offs. Notably, the Direct Alignment and Fusion scheme, when followed by an LLM-only fine-tuning stage dedicated to instruction following, achieved the highest performance on BLEU, ROUGE, and CIDEr metrics, despite not being the top performer in the initial pretraining phase. The secondbest performance was observed with the Joint Pretraining approach when augmented with an additional joint instruction tuning phase. Other hybrid or 'mix-and-match' fine-tuning strategies that were explored did not surpass the efficacy of these two leading methods. Consequently, based on these comprehensive results, our LSLM framework adopts the Direct Alignment and Fusion approach for initial gesture modality alignment, followed by an LLM-only instruction fine-tuning stage for the sign language recognition with instructions task. Illustrative translation samples from this configuration are presented in Fig. 4.

5. Ablation Study on LLM Backbone

We conduct several ablation studies to evaluate the effectiveness of Qwen2.5-3B-Instruct [49] as the LLM backbone for LSLM. We trained our model with the same learning rates and setup as mentioned in Sec 4.1.

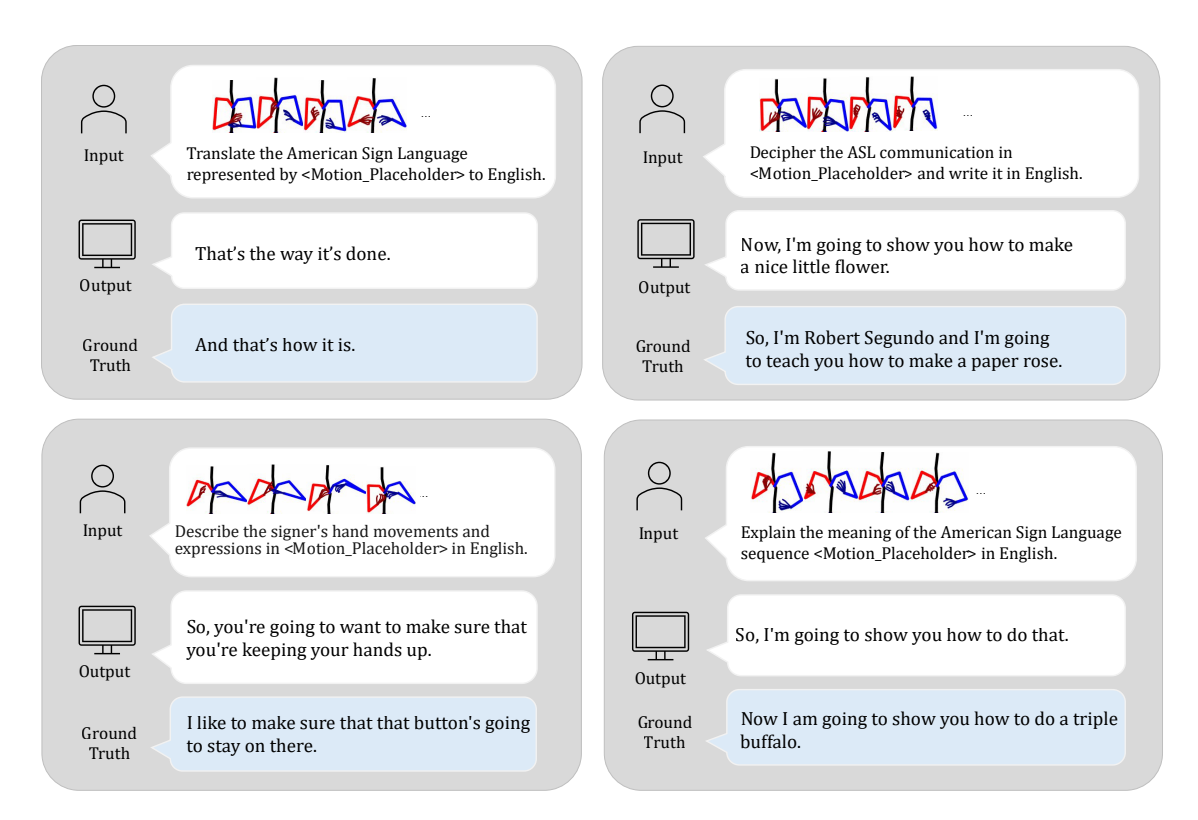


Figure 3. Instruction-guided Sign Language Recognition (SLR) examples from our LSLM framework. Each case shows the model's translation given a gesture sequence and prompt, alongside the ground truth. Outputs may slightly differ in wording but preserve the core meaning.

Table 5. Quantitative results for Qwen as LLM backbone for SLR during the pretraining stage. MLP: Direct Alignment and Fusion; MLP+LLM: Joint training; MLP/LLM: Staged training.

Methods	Pretraining	Bleu@1↑	Rouge↑	CIDEr↑
MotionGPT	-	7.9	8.3	2.5
Qwen (Direct Alignment and Fusion)	MLP	8.2	8.4	12.5
Qwen (Joint pretraining)	MLP+LLM	8.5	9.8	18.5

5.1. Pretraining

In the pretraining stage, we analyzed a Qwen-based backbone against the established baseline, with results detailed in Table 5. Similar to observations with the Llama backbone, employing Qwen led to notable improvements in fluency and content coverage, as indicated by higher BLEU and ROUGE scores. Furthermore, there was a clear enhancement in semantic similarity (e.g., CIDEr). However, when directly compared, the Qwen backbone did not surpass the performance levels achieved by the Llama backbone across the evaluated metrics, as shown in Table 6.

Regarding lexical accuracy, the Qwen backbone demonstrated a higher Word Error Rate (WER) compared to Llama. Further analysis of the generation patterns indicated that Qwen tended to produce more non-relevant words, resulting in a significantly higher insertion rate than observed with the

Llama-based model.

5.2. Instruction Tuning

In the instruction tuning phase, the Qwen backbone also demonstrated improved performance compared to the baseline, following similar trends observed with Llama as shown in Table 7. Specifically, when using Qwen, we achieved strong semantic similarity scores with the Direct Alignment and Fusion strategy for initial modality mapping, followed by LLM-only fine-tuning for instruction tuning. Alternatively, for better lexical accuracy, joint training during both the initial alignment and instruction fine-tuning stages produced favorable outcomes with the Owen backbone.

Consistent with patterns observed with the Llama backbone in Table 8, the Qwen-based LSLM achieved its highest semantic similarity scores using the Direct Alignment and Fusion strategy followed by LLM-only fine-tuning. Similar

Table 6. Comparison of LLM backbones for the Sign Language Recognition. MLP: Direct Alignment and Fusion; MLP+LLM: Joint training; MLP/LLM: Staged training.

Pretraining	Bleu@1↑	Bleu@4↑	Rouge↑	CIDEr↑	WER↓	Insertions↓	Deletions↓
MLP (Llama)	12.1	1.0	10.2	23.4	140	4.2	4.0
MLP+LLM (Llama)	13.6	1.5	11.7	26.9	114	4.0	1.7
MLP/LLM (Llama)	14.0	1.6	11.7	20.7	118	3.9	1.4
MLP (Qwen)	8.2	0.3	8.3	12.5	315	9.1	3.5
MLP+LLM (Qwen)	8.5	0.8	9.8	18.5	185	10.0	1.9

Table 7. Quantitative results for sign language recognition with instruction for Qwen as backbone. MLP: Direct Alignment and Fusion; MLP+LLM: Joint training.

Methods	Pretrained Modules	Instruction Tuning	Bleu@1↑	Rouge↑	CIDEr↑
MotionGPT	-	-	2.5	2.4	$5.7 \times e^{-4}$
Ours(Qwen)	MLP	LLM	10.2	11.2	22.3
Ours(Qwen)	MLP	MLP+LLM	10.0	11.1	18.6
Ours(Qwen)	MLP+LLM	LLM	12.9	11.5	15.1
Ours(Qwen)	MLP+LLM	MLP+LLM	13.2	11.8	15.1

to its pretraining performance, the Qwen-based model exhibited higher insertion rates. While this suggests a tendency toward generating more verbose translations, the model still maintained comparable lexical accuracy metrics in certain configurations.

6. Discussion

In this paper, we introduce the Large Sign Language Model (LSLM), a novel framework that successfully addresses 3D Sign Language translation for virtual communication. We solve this by pioneering the alignment of robust 3D sign gesture features, derived from the SMPL-X representations in 3D ASL datasets, with a Large Language Model backbone. This integration enables LSLM to achieve end-to-end translation of 3D American Sign Language, make initial attempts in direct gesture-to-text translation without traditional gloss intermediaries, and explore instruction-guided translation for greater output control, thereby enhancing translation accuracy for hearing-impaired individuals and advancing LLMs' capacity to understand complex, embodied multimodal communication.

Limitations and Broader Impacts. Large Language

Models (LLMs) face significant challenges and limitations when attempting to effectively understand sign language. Unlike spoken or written languages that LLMs excel at, sign languages are inherently visual-spatial, relying on handshapes, movements, facial expressions, and body posture to convey meaning. This multi-modal nature presents a substantial hurdle for current LLM architectures, which are primarily text-based. Another obstacle is the fundamental difference in data representation and the need for vision and pattern recognition capabilities to accurately interpret and translate the nuances of sign. Furthermore, unlike general motion datasets [43, 48], the relative scarcity of large, highquality, and diverse sign language datasets, compared to text or general motion data, hinders the training of robust LLMs. Overcoming these borders would ultimately pave the way for more inclusive and accessible technology for Deaf and hard-of-hearing communities. Future work could focus on expanding diverse 3D ASL datasets and developing linguistically-aware augmentation and learning strategies for models like LSLM.

Table 8. LLM Backbone comparison for SLR with instruction. MLP: Direct Alignment and Fusion; MLP+LLM: Joint training.

Backbone	Pretraining	Instruction Tuning	Bleu@1↑	Bleu@4↑	Rouge↑	CIDEr↑	WER↓	Insertions↓	Deletions↓
Llama	MLP	LLM	14.2	1.6	11.9	28.0	146	4.0	1.0
Llama	MLP	MLP+LLM	13.8	1.5	11.7	21.0	149	4.4	0.9
Llama	MLP+LLM	LLM	14.1	1.5	11.5	20.6	141	3.4	1.2
Llama	MLP+LLM	MLP+LLM	14.1	1.5	11.2	27.3	132	3.0	1.4
Qwen	MLP	LLM	10.2	1.2	11.2	22.3	195	10.1	1.0
Qwen	MLP	MLP+LLM	10.0	1.2	11.1	18.6	188	9.9	1.1
Qwen	MLP+LLM	LLM	12.9	1.9	11.5	15.1	149	5.1	0.8
Qwen	MLP+LLM	MLP+LLM	13.2	1.9	11.8	15.1	150	5.1	0.8

References

- [1] Telmo Adão, João Oliveira, Somayeh Shahrabadi, Hugo Jesus, Marco Fernandes, Angelo Costa, Vania Ferreira, Martinho Fradeira Gonçalves, Miguel A. Guevara Lopéz, Emanuel Peres, and Luís Gonzaga Magalhaes. Empowering deafhearing communication: Exploring synergies between predictive and generative ai-based strategies towards (portuguese) sign language interpretation. *Journal of Imaging*, 9(11), 2023. 1, 2, 5
- [2] Danielle Bragg, Oscar Koller, Mary Bellard, Larwan Berke, Patrick Boudreault, Annelies Braffort, Naomi Caselli, Matt Huenerfauth, Hernisa Kacorri, Tessa Verhoef, et al. Sign language recognition, generation, and translation: An interdisciplinary perspective. In *Proceedings of the 21st international* ACM SIGACCESS conference on computers and accessibility, pages 16–31, 2019. 2
- [3] Zhongang Cai, Wanqi Yin, Ailing Zeng, Chen Wei, Qingping Sun, Wang Yanjun, Hui En Pang, Haiyi Mei, Mingyuan Zhang, Lei Zhang, et al. Smpler-x: Scaling up expressive human pose and shape estimation. Advances in Neural Information Processing Systems, 36:11454–11468, 2023. 3
- [4] Necati Cihan Camgoz, Simon Hadfield, Oscar Koller, Hermann Ney, and Richard Bowden. Neural sign language translation. In 2018 IEEE/CVF Conference on Computer Vision and Pattern Recognition, pages 7784–7793, 2018. 12
- [5] Necati Cihan Camgoz, Oscar Koller, Simon Hadfield, and Richard Bowden. Sign language transformers: Joint end-to-end sign language recognition and translation. In *Proceedings of the IEEE/CVF conference on computer vision and pattern recognition*, pages 10023–10033, 2020. 2, 5
- [6] Qi Chang, Zhennan Yan, Mu Zhou, Di Liu, Khalid Sawalha, Meng Ye, Qilong Zhangli, Mikael Kanski, Subhi Al'Aref, Leon Axel, et al. Deeprecon: Joint 2d cardiac segmentation and 3d volume reconstruction via a structure-specific generative method. In *International Conference on Medical Image Computing and Computer-Assisted Intervention*, pages 567–577. Springer, 2022. 1
- [7] Eric M Chen, Di Liu, Sizhuo Ma, Michael Vasilkovsky, Bing Zhou, Qiang Gao, Wenzhou Wang, Jiahao Luo, Dimitris N Metaxas, Vincent Sitzmann, et al. Snapmoji: Instant generation of animatable dual-stylized avatars. arXiv preprint arXiv:2503.11978, 2025. 1
- [8] Runpeng Cui, Hu Liu, and Changshui Zhang. Recurrent convolutional neural networks for continuous sign language recognition by staged optimization. In *Proceedings of the IEEE conference on computer vision and pattern recognition*, pages 7361–7369, 2017. 2, 5
- [9] Zhenchao Cui, Wenbo Zhang, Zhaoxin Li, and Zhaoqi Wang. Spatial–temporal transformer for end-to-end sign language recognition. *Complex & Intelligent Systems*, 9(4):4645–4656, 2023. 1, 2, 5
- [10] Quan Dao, Khanh Doan, Di Liu, Trung Le, and Dimitris Metaxas. Improved training technique for latent consistency models. arXiv preprint arXiv:2502.01441, 2025.
- [11] Adrian C. Davis and Howard J. Hoffman. Hearing loss: rising prevalence and impact. *Bulletin of the World Health Organization*, 97(10):646–646A, 2019. 1

- [12] Son Nguyen Dinh, Tuan Dung Nguyen, Tri Tran, Nguyen Dang Huy Pham, Thuan Hieu Tran, Ngoc Anh Tong, Hoang Quang Huy, and Phi Le Nguyen. Sign Language Recognition: A Large-Scale Multi-View Dataset and Comprehensive Evaluation. In *Proceedings of the IEEE/CVF Winter Conference on Applications of Computer Vision (WACV)*, 2025. Published online 28 Feb 2025 by OpenReview, official proceedings details may vary slightly. 1
- [13] Amanda Duarte, Shruti Palaskar, Lucas Ventura, Deepti Ghadiyaram, Kenneth DeHaan, Florian Metze, Jordi Torres, and Xavier Giro-i Nieto. How2Sign: A Large-scale Multimodal Dataset for Continuous American Sign Language. In Conference on Computer Vision and Pattern Recognition (CVPR), 2021. 12
- [14] Yunhe Gao. Training like a medical resident: Context-prior learning toward universal medical image segmentation. In Proceedings of the IEEE/CVF Conference on Computer Vision and Pattern Recognition, pages 11194–11204, 2024.
- [15] Yunhe Gao, Di Liu, Zhuowei Li, Yunsheng Li, Dongdong Chen, Mu Zhou, and Dimitris N Metaxas. Show and segment: Universal medical image segmentation via in-context learning. In *Proceedings of the Computer Vision and Pattern Recognition Conference*, pages 20830–20840, 2025. 1
- [16] Jia Gong, Lin Geng Foo, Yixuan He, Hossein Rahmani, and Jun Liu. Llms are good sign language translators. In Proceedings of the IEEE/CVF Conference on Computer Vision and Pattern Recognition, pages 18362–18372, 2024. 1, 2, 3, 5
- [17] Chuan Guo, Shihao Zou, Xinxin Zuo, Sen Wang, Wei Ji, Xingyu Li, and Li Cheng. Generating diverse and natural 3d human motions from text. In 2022 IEEE/CVF Conference on Computer Vision and Pattern Recognition (CVPR), pages 5142–5151, 2022. 4
- [18] Chuan Guo, Xinxin Zuo, Sen Wang, and Li Cheng. Tm2t: Stochastic and tokenized modeling for the reciprocal generation of 3d human motions and texts. In *European Conference* on Computer Vision, pages 580–597. Springer, 2022. 3
- [19] Ligong Han, Song Wen, Qi Chen, Zhixing Zhang, Kunpeng Song, Mengwei Ren, Ruijiang Gao, Anastasis Stathopoulos, Xiaoxiao He, Yuxiao Chen, et al. Proxedit: Improving tuning-free real image editing with proximal guidance. In Proceedings of the IEEE/CVF Winter Conference on Applications of Computer Vision, pages 4291–4301, 2024. 1
- [20] Xiaoxiao He, Chaowei Tan, Bo Liu, Liping Si, Weiwu Yao, Liang Zhao, Di Liu, Qilong Zhangli, Qi Chang, Kang Li, et al. Dealing with heterogeneous 3d mr knee images: A federated few-shot learning method with dual knowledge distillation. In 2023 IEEE 20th International Symposium on Biomedical Imaging (ISBI), pages 1–5. IEEE, 2023.
- [21] Xiaoxiao He, Ligong Han, Quan Dao, Song Wen, Minhao Bai, Di Liu, Han Zhang, Martin Renqiang Min, Felix Juefei-Xu, Chaowei Tan, et al. Dice: Discrete inversion enabling controllable editing for multinomial diffusion and masked generative models. *arXiv preprint arXiv:2410.08207*, 2024. 1
- [22] Lianyu Hu, Liqing Gao, Zekang Liu, and Wei Feng. Self-Emphasizing Network for Continuous Sign Language Recognition. In *Proceedings of the AAAI Conference on Artificial Intelligence*, pages 1018–1026, 2023.

- [23] Jiayu Huang and Varin Chouvatut. Video-Based Sign Language Recognition via ResNet and LSTM Network. *Journal* of *Imaging*, 10(6):149, 2024. 1
- [24] Institut für Deutsche Gebärdensprache und Kommunikation Gehörloser. HamNoSys (Version 1997). Webpage, 1997. 12
- [25] Biao Jiang, Xin Chen, Wen Liu, Jingyi Yu, Gang Yu, and Tao Chen. Motiongpt: Human motion as a foreign language. Advances in Neural Information Processing Systems, 36, 2024. 1, 2, 3, 4, 5, 6
- [26] Jungeun Kim, Hyeongwoo Jeon, Jongseong Bae, and Ha Young Kim. Leveraging the power of mllms for gloss-free sign language translation. arXiv preprint arXiv:2411.16789, 2024. 1, 2, 5
- [27] Oscar Koller. Quantitative survey of the state of the art in sign language recognition. arXiv preprint arXiv:2008.09918, 2020. 1, 2, 5
- [28] D. Kumari and R. S. Anand. Isolated Video-Based Sign Language Recognition Using a Hybrid CNN-LSTM Framework Based on Attention Mechanism. *Electronics*, 13(7):1229, 2024.
- [29] Zhuowei Li, Zihao Xu, Ligong Han, Yunhe Gao, Song Wen, Di Liu, Hao Wang, and Dimitris N Metaxas. Implicit incontext learning. arXiv preprint arXiv:2405.14660, 2024.
- [30] Zhuowei Li, Long Zhao, Zizhao Zhang, Han Zhang, Di Liu, Ting Liu, and Dimitris N Metaxas. Steering prototypes with prompt-tuning for rehearsal-free continual learning. In Proceedings of the IEEE/CVF Winter Conference on Applications of Computer Vision, pages 2523–2533, 2024.
- [31] Zhuowei Li, Haizhou Shi, Yunhe Gao, Di Liu, Zhenting Wang, Yuxiao Chen, Ting Liu, Long Zhao, Hao Wang, and Dimitris N Metaxas. The hidden life of tokens: Reducing hallucination of large vision-language models via visual information steering. *arXiv* preprint arXiv:2502.03628, 2025. 1
- [32] Chin-Yew Lin. ROUGE: A package for automatic evaluation of summaries. In *Text Summarization Branches Out*, pages 74– 81, Barcelona, Spain, 2004. Association for Computational Linguistics. 5
- [33] Di Liu, Jiang Liu, Yihao Liu, Ran Tao, Jerry L Prince, and Aaron Carass. Label super resolution for 3d magnetic resonance images using deformable u-net. In *Medical Imaging* 2021: Image Processing, pages 606–611. SPIE, 2021. 1
- [34] Di Liu, Zhennan Yan, Qi Chang, Leon Axel, and Dimitris N Metaxas. Refined deep layer aggregation for multi-disease, multi-view & multi-center cardiac mr segmentation. In *Inter-national Workshop on Statistical Atlases and Computational Models of the Heart*, pages 315–322. Springer, 2021.
- [35] Di Liu, Yunhe Gao, Qilong Zhangli, Ligong Han, Xiaoxiao He, Zhaoyang Xia, Song Wen, Qi Chang, Zhennan Yan, Mu Zhou, et al. Transfusion: multi-view divergent fusion for medical image segmentation with transformers. In *International conference on medical image computing and computer-assisted intervention*, pages 485–495. Springer, 2022. 1
- [36] Di Liu, Anastasis Stathopoulos, Qilong Zhangli, Yunhe Gao, and Dimitris Metaxas. Lepard: Learning explicit part discovery for 3d articulated shape reconstruction. Advances in Neural Information Processing Systems, 36:54187–54198, 2023. 1

- [37] Di Liu, Xiang Yu, Meng Ye, Qilong Zhangli, Zhuowei Li, Zhixing Zhang, and Dimitris N Metaxas. Deformer: Integrating transformers with deformable models for 3d shape abstraction from a single image. In *Proceedings of the IEEE/CVF International Conference on Computer Vision*, pages 14236– 14246, 2023.
- [38] Di Liu, Long Zhao, Qilong Zhangli, Yunhe Gao, Ting Liu, and Dimitris N Metaxas. Deep deformable models: Learning 3d shape abstractions with part consistency. *arXiv preprint arXiv:2309.01035*, 2023.
- [39] Di Liu, Bingbing Zhuang, Dimitris N Metaxas, and Manmohan Chandraker. Instantaneous perception of moving objects in 3d. In *Proceedings of the IEEE/CVF conference on computer vision and pattern recognition*, pages 19573–19583, 2024.
- [40] Di Liu, Teng Deng, Giljoo Nam, Yu Rong, Stanislav Pidhorskyi, Junxuan Li, Jason Saragih, Dimitris N Metaxas, and Chen Cao. Lucas: Layered universal codec avatars. In Proceedings of the Computer Vision and Pattern Recognition Conference, pages 21127–21137, 2025. 1
- [41] Ilya Loshchilov and Frank Hutter. Decoupled weight decay regularization. In *International Conference on Learning Representations*, 2017. 5
- [42] Jiahao Luo, Chaoyang Wang, Michael Vasilkovsky, Vladislav Shakhrai, Di Liu, Peiye Zhuang, Sergey Tulyakov, Peter Wonka, Hsin-Ying Lee, James Davis, and Jian Wang. T2bs: Text-to-character blendshapes via video generation. In Proceedings of the IEEE/CVF International Conference on Computer Vision (ICCV), pages 13625–13637, 2025.
- [43] Naureen Mahmood, Nima Ghorbani, Nikolaus F. Troje, Gerard Pons-Moll, and Michael J. Black. AMASS: Archive of motion capture as surface shapes. In *International Conference on Computer Vision*, pages 5442–5451, 2019. 8
- [44] Carlos Martín-Isla, Víctor M Campello, Cristian Izquierdo, Kaisar Kushibar, Carla Sendra-Balcells, Polyxeni Gkontra, Alireza Sojoudi, Mitchell J Fulton, Tewodros Weldebirhan Arega, Kumaradevan Punithakumar, et al. Deep learning segmentation of the right ventricle in cardiac mri: the m&ms challenge. IEEE Journal of Biomedical and Health Informatics, 27(7):3302–3313, 2023. 1
- [45] Meta AI. Llama 3.2: Revolutionizing edge ai and vision with open, customizable models. Blog Post, 2024. Accessed: 2025-05-12. 5
- [46] Kishore Papineni, Salim Roukos, Todd Ward, and Wei-Jing Zhu. Bleu: a method for automatic evaluation of machine translation. In *Proceedings of the 40th Annual Meeting of* the Association for Computational Linguistics, pages 311– 318, Philadelphia, Pennsylvania, USA, 2002. Association for Computational Linguistics. 5
- [47] Georgios Pavlakos, Vasileios Choutas, Nima Ghorbani, Timo Bolkart, Ahmed A. A. Osman, Dimitrios Tzionas, and Michael J. Black. Expressive body capture: 3D hands, face, and body from a single image. In *Proceedings IEEE Conf.* on Computer Vision and Pattern Recognition (CVPR), pages 10975–10985, 2019. 1
- [48] Matthias Plappert, Christian Mandery, and Tamim Asfour. The KIT motion-language dataset. *Big Data*, 4(4):236–252, 2016. 8

- [49] Qwen, :, An Yang, Baosong Yang, Beichen Zhang, Binyuan Hui, Bo Zheng, Bowen Yu, Chengyuan Li, Dayiheng Liu, Fei Huang, Haoran Wei, Huan Lin, Jian Yang, Jianhong Tu, Jianwei Zhang, Jianxin Yang, Jiaxi Yang, Jingren Zhou, Junyang Lin, Kai Dang, Keming Lu, Keqin Bao, Kexin Yang, Le Yu, Mei Li, Mingfeng Xue, Pei Zhang, Qin Zhu, Rui Men, Runji Lin, Tianhao Li, Tianyi Tang, Tingyu Xia, Xingzhang Ren, Xuancheng Ren, Yang Fan, Yang Su, Yichang Zhang, Yu Wan, Yuqiong Liu, Zeyu Cui, Zhenru Zhang, and Zihan Qiu. Qwen2.5 technical report, 2025. 6
- [50] Hamid Ranjbar and Ahmad Taheri. Continuous Sign Language Recognition Using Intra-inter Gloss Attention, 2024.
- [51] Aaron Van Den Oord, Oriol Vinyals, et al. Neural discrete representation learning. Advances in neural information processing systems, 30, 2017. 3
- [52] Ramakrishna Vedantam, C. Lawrence Zitnick, and Devi Parikh. CIDEr: Consensus-based Image Description Evaluation. In *Proceedings of the IEEE Conference on Computer Vision and Pattern Recognition (CVPR)*, pages 4566–4575, Boston, MA, USA, 2015. 5
- [53] Yuan Wang, Di Huang, Yaqi Zhang, Wanli Ouyang, Jile Jiao, Xuetao Feng, Yan Zhou, Pengfei Wan, Shixiang Tang, and Dan Xu. Motiongpt-2: A general-purpose motion-language model for motion generation and understanding. arXiv preprint arXiv:2410.21747, 2024. 1, 3
- [54] Song Wen, Hao Wang, Di Liu, Qilong Zhangli, and Dimitris Metaxas. Second-order graph odes for multi-agent trajectory forecasting. In Proceedings of the IEEE/CVF Winter Conference on Applications of Computer Vision, pages 5101–5110, 2024. 1
- [55] Zhaoyang Xia, Somdeb Sarkhel, Mehrab Tanjim, Stefano Petrangeli, Ishita Dasgupta, Yuxiao Chen, Jinxuan Xu, Di Liu, Saayan Mitra, and Dimitris N Metaxas. Visiar: Empower mllm for visual story ideation. In Findings of the Association for Computational Linguistics: ACL 2025, pages 18384–18402, 2025. 1
- [56] Zhengdi Yu, Shaoli Huang, Yongkang Cheng, and Tolga Birdal. Signavatars: A large-scale 3d sign language holistic motion dataset and benchmark. In *Proceedings of the Euro*pean Conference on Computer Vision (ECCV), pages 1–19, 2024. 1, 4
- [57] Yanchi Zhang and Xianwei Jiang. Recent advances on deep learning for sign language recognition. *Computer Modeling in Engineering & Sciences*, 139(3):2399–2450, 2024. 1
- [58] Qilong Zhangli, Jingru Yi, Di Liu, Xiaoxiao He, Zhaoyang Xia, Qi Chang, Ligong Han, Yunhe Gao, Song Wen, Haiming Tang, et al. Region proposal rectification towards robust instance segmentation of biological images. In *International Conference on Medical Image Computing and Computer-Assisted Intervention*, pages 129–139. Springer, 2022. 1
- [59] Qilong Zhangli, Jindong Jiang, Di Liu, Licheng Yu, Xiaoliang Dai, Ankit Ramchandani, Guan Pang, Dimitris N Metaxas, and Praveen Krishnan. Layout-agnostic scene text image synthesis with diffusion models. In 2024 IEEE/CVF Conference on Computer Vision and Pattern Recognition (CVPR), pages 7496–7506. IEEE Computer Society, 2024. 1

- [60] Qilong Zhangli, Di Liu, Abhishek Aich, Dimitris Metaxas, and Samuel Schulter. Resolving inconsistent semantics in multi-dataset image segmentation. arXiv preprint arXiv:2409.09893, 2024.
- [61] Jiangbin Zheng, Yile Wang, Cheng Tan, Siyuan Li, Ge Wang, Jun Xia, Yidong Chen, and Stan Z. Li. CVT-SLR: Contrastive Visual-Textual Transformation for Sign Language Recognition with Variational Alignment. In Proceedings of the IEEE/CVF Conference on Computer Vision and Pattern Recognition (CVPR), pages 14977–14987, 2023.
- [62] Ronglai Zuo, Zekang Liu, Lianyu Hu, Jiangbin Zheng, Liqing Gao, Fangyun Wei, and Brian Mak. Towards Online Continuous Sign Language Recognition and Translation. In *Proceed*ings of the 2024 Conference on Empirical Methods in Natural Language Processing (EMNLP). Association for Computational Linguistics, 2024. Page numbers may vary with final publication; check ACL Anthology for updates. 1

Supplementary Material for Large Sign Language Models: Toward 3D American Sign Language Translation

A. Implementation details

A.1. Training Hyperparameters

Key hyperparameters for our model training are as follows:

Table 9. Training Hyperparameters

Component	Hyperparameter	Value/Type
	Codebook Size	1024
	Optimizer	AdamW
Gesture Tokenizer (VQ-VAE)	Learning Rate	2×10^{-4}
	Batch Size	256
	Number of Joints	52
	Max Token Length	250
TTM - AP	Batch Size per GPU	16
LLM + Alignment	Alignment MLP LR	1×10^{-6}
	LLM Fine-tune LR	5×10^{-7}
Motion Token IDs	LLaMA	128259
	Qwen	151668

A.2. Dataset Detail

The details of the SignAvatar dataset are listed below:

Table 10. Number of samples in SignAvatars dataset.

Dataset samples	Dev	Test	Val	Language
How2Sign [13]	24476	3060	3059	American Sign Language (ASL)
HamNoSys [24]	4588	574	573	Sign Transcriptive System
RWTH-PHOENIX-Weather [4]	2667	334	333	Germany Sign Language (DGS)

A.3. Dataset Detail

The details of the SignAvatar dataset are listed in List 1.

B. More Qualitative Results

We show more results from our LSLM with Qwen backbone in Fig 4.

Listing 1. Templates used for pretraining and instruction-tuning.

```
// Pretraining Template
     "Motion-to-Text": {
        "m2t": {
    "class": "m2t",
          "input": [
             "<Motion_Placeholder>"
           "output": [
             "<Caption_Placeholder>"
10
11
12
     }
14 }
15
16 {
     // Instruction-Tuning Template
17
     "Motion-to-Text": {
18
        "caption": {
    "class": "m2t",
19
20
          "input": [
21
  "Translate the American Sign Language represented by <Motion_Placeholder> to English.", "Decipher the ASL communication in <Motion_Placeholder> and write it in English.",
   "Rephrase the American Sign Language in <Motion_Placeholder> as spoken English.",
   "Explain the meaning of the American Sign Language sequence <Motion_Placeholder> in English.",
26 . . .
          28
             "<Caption_Placeholder>"
31
    }
32
33 }
```

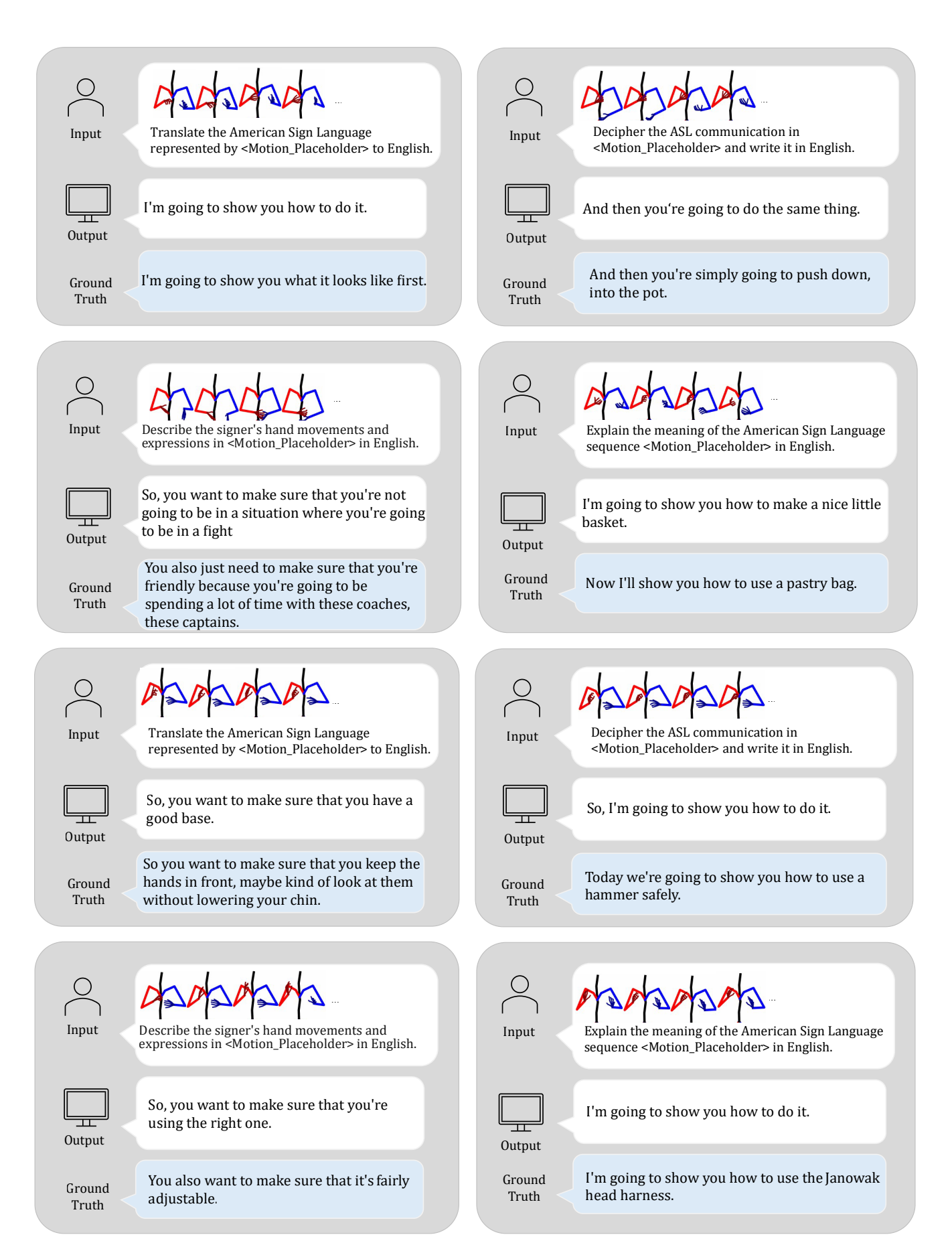


Figure 4. Instruction-guided Sign Language Recognition (SLR) examples from our LSLM framework with Qwen backbone. Each case shows the model's translation given a gesture sequence and prompt, alongside the ground truth. Outputs may slightly differ in wording but preserve the core meaning.